

STUDY ON DECOUPLED PROJECTION METHOD FOR CAHN–HILLIARD EQUATION

GYEONGGYU LEE¹ AND SEUNGGYU LEE^{2,3,†}

¹NATIONAL INSTITUTE FOR MATHEMATICAL SCIENCES, REPUBLIC OF KOREA
Email address: sso55787@nims.re.kr

²DIVISION OF APPLIED MATHEMATICAL SCIENCES, KOREA UNIVERSITY, REPUBLIC OF KOREA

³BIOMEDICAL MATHEMATICS GROUP, INSTITUTE FOR BASIC SCIENCE, REPUBLIC OF KOREA
Email address: †sky509@korea.ac.kr

ABSTRACT. We study the numerical analysis for the Cahn–Hilliard (CH) equation using the decoupled projection (DP) method. The CH equation is a fourth order nonlinear partial differential equation that is hard to solve. Therefore, various of numerical schemes have been proposed to solve the CH equation. To verify the relation of each existing scheme for the CH equation, we consider the DP method for linear convex splitting schemes. We present the numerical experiments to demonstrate our analysis. Throughout this study, it is expected to construct a novel numerical scheme using the relation with existing numerical schemes.

1. INTRODUCTION

The Cahn–Hilliard (CH) equation is a fourth order partial difference equation which has non-linear term and biharmonic term. The CH equation was originated from the spinodal decomposition in a binary alloy which is a kind of the phase separation [1, 2]. The CH equation is as follows :

$$\begin{aligned}\frac{\partial\phi(\mathbf{x}, t)}{\partial t} &= \Delta\mu(\mathbf{x}, t), \quad \mathbf{x} \in \Omega, t \in (0, T), \\ \mu(\mathbf{x}, t) &= F'(\phi(\mathbf{x}, t)) - \epsilon^2\Delta\phi(\mathbf{x}, t)\end{aligned}$$

where $\Omega \subset \mathbb{R}^d$ for $d = 1, 2, 3$ is a domain, and ϵ is a positive constant which is related to interfacial energy. In addition, T is a final time and Δ is the Laplace operator. Moreover, ϕ is the scalar field which is difference between the concentration of the binary alloys and μ is a chemical potential [3]. To make it easier to describe, we will denote $\phi(\mathbf{x}, t)$ as ϕ . In addition, μ is written in a same manner. Moreover, $F(\phi) = 0.25(\phi^2 - 1)^2$ is the Helmholtz free energy

Received November 15 2023; Revised December 8 2023; Accepted in revised form December 11 2023; Published online December 25 2023.

2000 *Mathematics Subject Classification.* 65M12.

Key words and phrases. Cahn–Hilliard equation, Decoupled projection method, Energy stability.

† Corresponding author.

which has a double well potential. The CH equation has the homogeneous Neumann condition which is called the no flux boundary condition. it is given as follows:

$$\frac{\partial \phi}{\partial \mathbf{n}} = \frac{\partial \mu}{\partial \mathbf{n}} = 0 \text{ on } \partial \Omega.$$

where \mathbf{n} is the outward normal vector on $\partial \Omega$. We denote that $\partial \phi / \partial \mathbf{n} = \mathbf{n} \cdot \nabla \phi$.

The CH equation has been widely applied to various scientific fields such as image segmentation, volume reconstruction, tumor growth simulation, topology optimization [4]. However, because it is difficult to solve, one of main scientific topic for the CH equation is construction of the numerical scheme which is unconditional stable, accurate, and convenient for the implementation. Therefore, various of numerical schemes have been proposed to solve the CH equation. In this work, we consider some convex splitting methods and the decoupled projection method. The decoupled projection (DP) method is a fractional step method which uses the block LU decomposition and the linear approximation [5]. Because the main purpose is constructing it more convenient to implement, the DP method was treated with the complex governing equation such the incompressible NS equation and natural convection model [7, 8]. In addition, the convex splitting methods are constructed based on the contractive and expansive parts of the free energy of a governing equation [6]. Furthermore, the constructed numerical scheme can be unconditionally energy-gradient stable by the properties of convexity and concavity. The stability means that the proposed numerical schemes are satisfying the total energy dissipation law for any time step δt [3].

The contents this paper are as follows. In Section 2, we present some proof of properties for the CH equation. Numerical analysis is concerned in Section 3. Numerical simulations are presented in Section 4. The conclusion is given in Section 5.

2. GOVERNING EQUATION

In this section, we present some properties of the CH equation which are the gradient flow, the total energy dissipation, and the total mass preserving. To prove the properties, we use the integration by part with the no flux boundary condition.

Definition 2.1. *We define the following inner products:*

- (i) $(u, v)_2 = \int_{\Omega} uv d\mathbf{x}$.
- (ii) $(u, v)_{H^{-1}} = (\nabla u, \nabla v)_2 = (u, -\Delta v)_2$.

Theorem 2.2. *The CH equation is the H^{-1} gradient flow of the Ginzburg–Landau free energy functional*

$$\mathcal{E}(\phi) = \int_{\Omega} \left(F(\phi) + \frac{\epsilon^2}{2} |\nabla \phi|^2 \right) d\mathbf{x}.$$

The CH equation is derived as follows:

$$\phi_t = -\text{grad} \mathcal{E}(\phi) = \Delta \left(\frac{\delta \mathcal{E}(\phi)}{\delta \phi} \right).$$

Proof. For every $v \in C_c^\infty(\Omega)$,

$$\frac{\delta \mathcal{E}(\phi)}{\delta \phi} = \left. \frac{d}{d\theta} \mathcal{E}(\phi + \theta v) \right|_{\theta=0} = \lim_{\theta \rightarrow 0} \frac{1}{\theta} (\mathcal{E}(\phi + \theta v) - \mathcal{E}(\phi)) = \int_{\Omega} (F'(\phi) - \epsilon^2 \Delta \phi) v d\mathbf{x}, \quad (2.1)$$

where $\delta \mathcal{E}(\phi)/\delta \phi = F'(\phi) - \epsilon^2 \Delta \phi$ is the variational derivative. Put $-\Delta \phi_v$ instead of v in Eq. (2.1). Then,

$$\begin{aligned} \int_{\Omega} (F'(\phi) - \epsilon^2 \Delta \phi) v d\mathbf{x} &= \int_{\Omega} -\Delta \phi_v (F'(\phi) - \epsilon^2 \Delta \phi) d\mathbf{x} = \int_{\Omega} \nabla (F'(\phi) - \epsilon^2 \Delta \phi) \cdot \nabla \phi_v d\mathbf{x} \\ &= (\nabla (F'(\phi) - \epsilon^2 \Delta \phi), \nabla \phi_v)_2 = (-\Delta (F'(\phi) - \epsilon^2 \Delta \phi), \phi_v)_2 \\ &= (F'(\phi) - \epsilon^2 \Delta \phi, \phi_v)_{H^{-1}}. \end{aligned}$$

Because the ϕ_v is chosen as the test function, we can say that $\text{grad} \mathcal{E}(\phi) = -\Delta (F'(\phi) - \epsilon^2 \Delta \phi)$. \square

Theorem 2.3. *The CH equation is satisfying the total energy dissipation law:*

$$\frac{d}{dt} \mathcal{E}(\phi) \leq 0.$$

Proof. When differentiating the energy functional $\mathcal{E}(\phi)$ with respect to time t , we can derive as follows:

$$\begin{aligned} \frac{d}{dt} \mathcal{E}(\phi) &= \int_{\Omega} (F'(\phi) - \epsilon^2 \Delta \phi) \phi_t d\mathbf{x} = \int_{\Omega} (F'(\phi) - \epsilon^2 \Delta \phi) \Delta (F'(\phi) - \epsilon^2 \Delta \phi) d\mathbf{x} \\ &= \int_{\partial \Omega} (\mathbf{n} \cdot \nabla (F'(\phi) - \epsilon^2 \Delta \phi)) (F'(\phi) - \epsilon^2 \Delta \phi) d\mathbf{S} - \int_{\Omega} |\nabla (F'(\phi) - \epsilon^2 \Delta \phi)|^2 d\mathbf{x} \\ &= - \int_{\Omega} |\nabla (F'(\phi) - \epsilon^2 \Delta \phi)|^2 d\mathbf{x} \leq 0. \end{aligned}$$

Therefore, the CH equation is satisfying the energy dissipation law. \square

Theorem 2.4. *The CH equation is satisfying the mass preserving property:*

$$\frac{d}{dt} \int_{\Omega} \phi d\mathbf{x} = 0.$$

Proof. It can be proved using the divergence theorem and the homogeneous Neumann boundary condition,

$$\frac{d}{dt} \int_{\Omega} \phi d\mathbf{x} = \int_{\Omega} \phi_t d\mathbf{x} = \int_{\Omega} \Delta \mu d\mathbf{x} = \int_{\partial \Omega} \mathbf{n} \cdot \nabla \mu dS = 0.$$

Therefore, the total mass of the CH equation is preserved with time. \square

3. NUMERICAL ANALYSIS

In this section, we discuss about the DP method for some unconditional gradient stable schemes which are based on the linear convex splitting scheme. To discuss these numerical schemes, let us consider the following numerical scheme:

$$\begin{aligned}\frac{\phi^{n+1} - \phi^n}{\delta t} &= \Delta \mu^{n+1}, \\ \mu^{n+1} &= f^n + \alpha (\phi^{n+1} - \phi^n) - \epsilon^2 \Delta \phi^{n+1}\end{aligned}\quad (3.1)$$

where ϕ^n is a numerical approximation of the ϕ at time $n\delta t$. In addition, μ^n is used in a same manner. For simplicity, we use f^n as $F'(\phi^n)$. δt is used as the time step and α is chosen in the closed interval $[0, 2]$. The considered numerical scheme is called as the semi implicit Euler's (SI) one for $\alpha = 0$. Moreover, for $\alpha = 2$, the considered numerical scheme is the linear stabilized splitting (LSS) one. In this case, the numerical scheme is satisfying the unique solvability, unconditionally energy gradient stable where ϕ is belong in the closed interval $[-1, 1]$ [2]. For space discretization, we use the Fourier spectral method which is almost exact for space. The matrix formula for Eq. (3.1) can be written as follows:

$$\begin{pmatrix} \mathbf{I} & -\delta t \Delta \\ \epsilon^2 \Delta - \alpha \mathbf{I} & \mathbf{I} \end{pmatrix} \begin{pmatrix} \phi^{n+1} \\ \mu^{n+1} \end{pmatrix} = \begin{pmatrix} \phi^n \\ f^n - \alpha \phi^n \end{pmatrix}. \quad (3.2)$$

Here, \mathbf{I} is the identity operator. That is, $\mathbf{I}(\phi) = \phi$. Using the LU decomposition, we can factorize Eq. (3.2) as follows:

$$\begin{pmatrix} \mathbf{I} & 0 \\ \epsilon^2 \Delta & \mathbf{I} \end{pmatrix} \begin{pmatrix} \mathbf{I} & -\delta t \Delta \\ 0 & \mathbf{I} + \delta t \Delta (\epsilon^2 \Delta - \alpha \mathbf{I}) \end{pmatrix} \begin{pmatrix} \phi^{n+1} \\ \mu^{n+1} \end{pmatrix} = \begin{pmatrix} \phi^n \\ f^n - \alpha \phi^n \end{pmatrix}.$$

Let us consider that

$$\begin{pmatrix} \mathbf{I} & -\delta t \Delta \\ 0 & \mathbf{I} + \delta t \Delta (\epsilon^2 \Delta - \alpha \mathbf{I}) \end{pmatrix} \begin{pmatrix} \phi^{n+1} \\ \mu^{n+1} \end{pmatrix} = \begin{pmatrix} \phi^* \\ \mu^* \end{pmatrix}. \quad (3.3)$$

Then, we have that

$$\begin{pmatrix} \mathbf{I} & 0 \\ \epsilon^2 \Delta & \mathbf{I} \end{pmatrix} \begin{pmatrix} \phi^* \\ \mu^* \end{pmatrix} = \begin{pmatrix} \phi^n \\ f^n - \alpha \phi^n \end{pmatrix}. \quad (3.4)$$

Equation (3.4) can be rewritten as

$$\begin{aligned}\phi^* &= \phi^n, \\ \mu^* &= -\epsilon^2 \Delta \phi^* + f^n - \alpha \phi^n.\end{aligned}$$

In other words, μ^* is $f^n - (\epsilon^2 \Delta + \alpha) \phi^n$ and ϕ^* is ϕ^n . In addition, Eq. (3.3) can be written as

$$\begin{aligned}\phi^{n+1} &= \phi^* + \delta t \Delta \mu^*, \\ \mu^{n+1} &= [\mathbf{I} + \delta t \Delta (\epsilon^2 \Delta - \alpha \mathbf{I})]^{-1} \mu^*.\end{aligned}\quad (3.5)$$

Because $\phi^* = \phi^n$ and $\mu^* = f^n - (\epsilon^2 \Delta + \alpha) \phi^n$, the numerical scheme (3.5) can be rewritten as the following numerical procedure:

$$\begin{aligned}\mu^* &= f^n - (\epsilon^2 \Delta + \alpha) \phi^n, \\ \mu^{n+1} &= [\mathbf{I} + \delta t \Delta (\epsilon^2 \Delta - \alpha \mathbf{I})]^{-1} \mu^*, \\ \phi^{n+1} &= \phi^n + \delta t \Delta \mu^*.\end{aligned}$$

Theorem 3.1. *The considered numerical scheme for the CH equation is satisfying the mass preserving property:*

$$\int_{\Omega} \phi^{n+1} d\mathbf{x} = \int_{\Omega} \phi^n d\mathbf{x}$$

for every positive integer n .

Proof. It can be proved using the divergence theorem and the homogeneous Neumann boundary condition,

$$\int_{\Omega} \phi^{n+1} d\mathbf{x} = \int_{\Omega} \phi^n d\mathbf{x} + \delta t \int_{\Omega} \Delta \mu^* d\mathbf{x} = \int_{\Omega} \phi^n d\mathbf{x} + \delta t \int_{\partial\Omega} \mathbf{n} \cdot \nabla \mu^* dS = \int_{\Omega} \phi^n d\mathbf{x}.$$

Therefore, the total mass of the CH equation is preserved with time. \square

Remark 3.2. *For $\beta = \alpha \delta t$, the numerical scheme (3.1) can be written as follows,*

$$\frac{\phi^{n+1} - \phi^n}{\delta t} = \Delta \left(f^n + \beta \left(\frac{\phi^{n+1} - \phi^n}{\delta t} \right) - \epsilon^2 \Delta \phi^{n+1} \right). \quad (3.6)$$

Let us consider the viscous CH equation:

$$(1 - \gamma) \frac{\partial \phi}{\partial t} = \Delta \left(F'(\phi) + \gamma \frac{\partial \phi}{\partial t} - \epsilon^2 \Delta \phi \right) \quad (3.7)$$

where γ is the real valued constant belong to closed interval $[0, 1]$. Let $\tau = t/(1 - \gamma)$ and $\nu = \gamma/(1 - \gamma)$. Then, Eq. (3.7) can be rewritten for τ ,

$$\frac{\partial \phi(\mathbf{x}, \tau)}{\partial \tau} = \Delta \left(F'(\phi(\mathbf{x}, \tau)) + \nu \frac{\partial \phi(\mathbf{x}, \tau)}{\partial \tau} - \epsilon^2 \Delta \phi(\mathbf{x}, \tau) \right).$$

For the viscous CH equation, let us consider the semi implicit Euler's scheme,

$$\frac{\phi^{n+1} - \phi^n}{\delta \tau} = \Delta \left(f^n + \nu \left(\frac{\phi^{n+1} - \phi^n}{\delta \tau} \right) - \epsilon^2 \Delta \phi^{n+1} \right). \quad (3.8)$$

When ν and $\delta \tau$ are considered as β and δt each other, we can obtain that the Eq. (3.6) and (3.8) are equivalent. From the results, we can observe that the linear convex splitting schemes for the CH equation have the relation with the viscous CH equation.

4. NUMERICAL EXPERIMENT

In this section, we present some numerical experiments to observe some properties of the proposed numerical scheme for the CH equation in Fig. 1 and 2 which are temporal accuracy, spatial accuracy, mass preserving, and energy dissipation. Moreover, the effect of viscosity γ is also presented in Fig. 3. We use the computational domain $\Omega = (0, 1)$ in Fig. 1 and $\Omega = (0, 1)^2$ in two dimensional (2D) space to perform the numerical experiment in Fig. 2–3. Moreover, $\epsilon_m = mh / (2\sqrt{2} \tanh^{-1}(0.9))$.

To confirm the accuracy of the considered numerical schemes, we perform the numerical test in 1D space. Because the CH equation does not have the exact solution, we use the reference solution using the sufficiently small time step δt in temporal accuracy and the grid size h for spatial accuracy. Here, the initial condition $\cos(2\pi x)$ is used. In addition, to measure the error, we use the l_2 error. That is, $\|e\|_2 = \sqrt{\sum_{i=1}^{N_x} e_i^2}$ where e is difference between numerical solution and exact solution and e_i is numerical approximation at i -th node. Here, the grid size h is 2^{-7} . the interface thickness ϵ and the final time T are used as ϵ_4 and 0.0048 each other. The reference solution is considered with the time step $\delta t_{ref} = 2^{-21}$. In Figure 1(a), the time step δt is used as 2^m for $m = -20, \dots, -3$. From the Fig. 1(a), we can observe that the considered schemes have the first order accuracy for the time. Moreover, to concern the spatial accuracy, we use the time step $\delta t = 2^{-20}$, total iteration $N_t = 40000$, $\epsilon = 0.01$ in Fig. 1(b). The reference solution is considered with the grid size $h_{ref} = 2^{-8}$. In Figure 1(b), the grid size h is used as 2^m for $m = -8, \dots, -1$. Figure 1(b) presents that the considered schemes have the spectral order accuracy for the space. We can say that the DP method keeps for the accuracy in time and space each other from the Fig. 1. To present the mass preserving and energy stability in Fig. 2, let us define the discrete mass \mathcal{M}_h^n and discrete energy \mathcal{E}_h^n in 2D space each other:

$$\mathcal{M}_h^n = h^2 \sum_{j=1}^{N_y} \sum_{i=1}^{N_x} \phi_{ij}^n,$$

$$\mathcal{E}_h^n = h^2 \left[\sum_{j=1}^{N_y} \sum_{i=1}^{N_x} F(\phi_{ij}^n) + \frac{\epsilon^2}{2} \sum_{j=1}^{N_y-1} \sum_{i=1}^{N_x} \left(\frac{\phi_{i,j+1}^n - \phi_{ij}^n}{h} \right)^2 + \frac{\epsilon^2}{2} \sum_{j=1}^{N_y} \sum_{i=1}^{N_x-1} \left(\frac{\phi_{i+1,j}^n - \phi_{ij}^n}{h} \right)^2 \right]$$

where ϕ_{ij}^n is the numerical approximation at i -th node and j -th node in x -, y -directions each other. The initial condition is used as $0.1 \text{rand}(x, y)$ where $\text{rand}(x, y)$ is random valued function between -1 and 1 . Here, the number of grid N_x , N_y and grid size h are considered as $N_x = N_y = 128$ and $h = 1/128$. The time step δt and the total iteration time N_t are used as $30h^2$ and 300 each other. Moreover, the interfacial thickness ϵ is used as $\epsilon_1 6$. We describe the considered original schemes as the line and the considered schemes with the DP method as shapes where α are chosen as 0, 1, and 2. The black, red, and blue ones are present for $\alpha = 0, 1, 2$ in Fig. 2. Figure 2(a) presents the discrete total mass \mathcal{M}_h^n at each time using the considered numerical schemes. From Fig. 2(a), we have that the all of the used scheme satisfying the mass preserving property. Moreover, we present the snapshot at time 0, $150\delta t$, and $300\delta t$ which

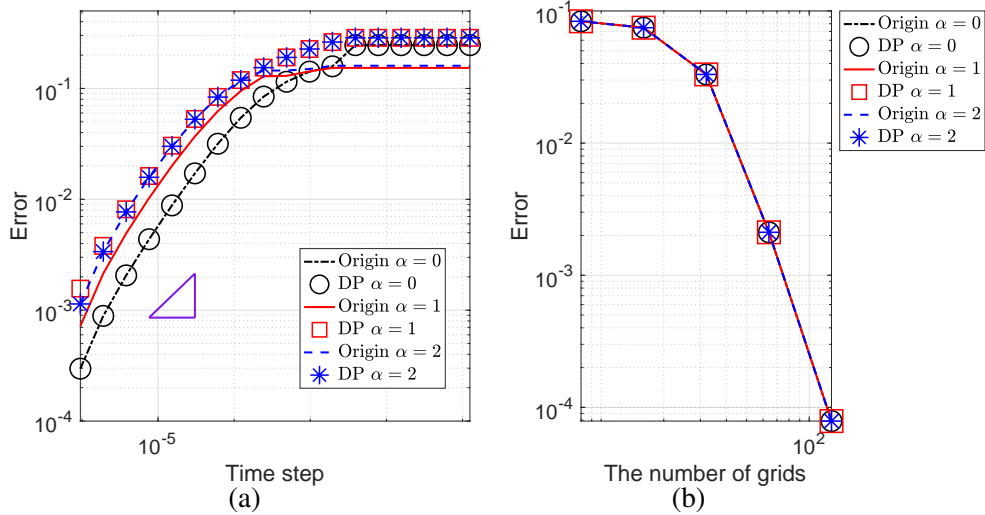


FIGURE 1. (a) is temporal error, (b) is spatial error.

present the phase separation in 2D space. In addition, Fig. 2(b) shows the normalized total discrete energy $\mathcal{E}_h^n/\mathcal{E}_h^1$ at each time. From Fig. 2(b), we can concerned that the considered numerical scheme satisfying the unconditionally gradient stable.

In Fig. 3, we consider the following initial condition $\phi_0(x, y)$:

$$\begin{aligned} \phi_0(x, y) = & \tanh \left(\frac{0.11 - \sqrt{(x - 0.38)^2 + (y - 0.5)^2}}{\sqrt{2}\epsilon} \right) \\ & + \tanh \left(\frac{0.11 - \sqrt{(x - 0.62)^2 + (y - 0.5)^2}}{\sqrt{2}\epsilon} \right) + 1. \end{aligned}$$

The initial condition is described in Fig. 3(a). Here, the number of grid $N_x = N_y$ are chosen as 200, the mesh size $h = 1/N_x = 1/N_y$, $\epsilon = \epsilon_{16}$. In addition, the time step δt is used as h^2 and the total iteration time is used as 500. Figure 3(b)–(c) present the numerical result for the viscous CH equation at time $500\delta t$ using the viscosity $\gamma = 0.1, \gamma = 0.01, \gamma = 0.001$, and $\gamma = 0$, respectively. When we consider the small γ , the dynamics is more faster then the large one in Fig. 3.

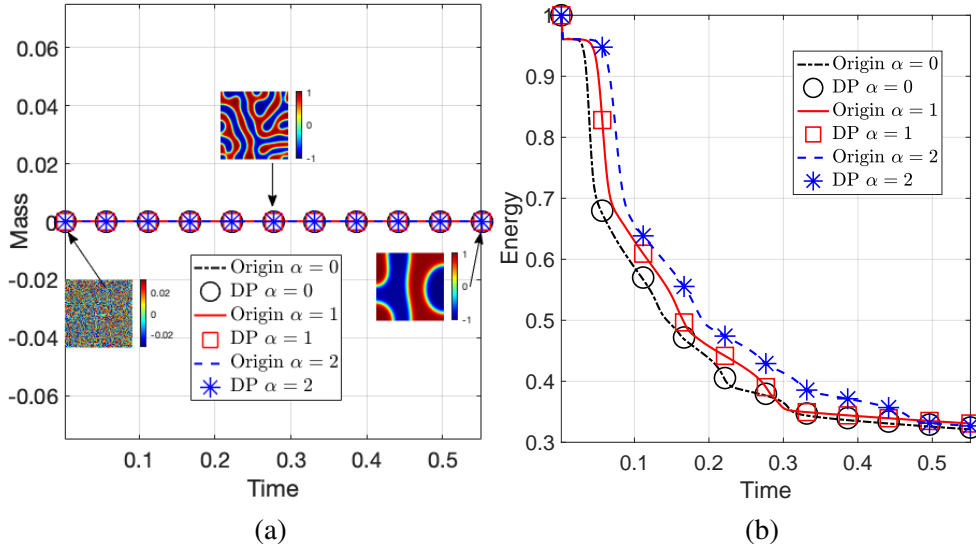


FIGURE 2. (a) is total discrete mass, (b) is total discrete energy. Time step δt and total iteration N_t are $30h^2$ and 300 each other. Dynamics are presented at time $0\delta t, 150\delta t, \text{ and } 300\delta t$ in mini snapshots of (a).

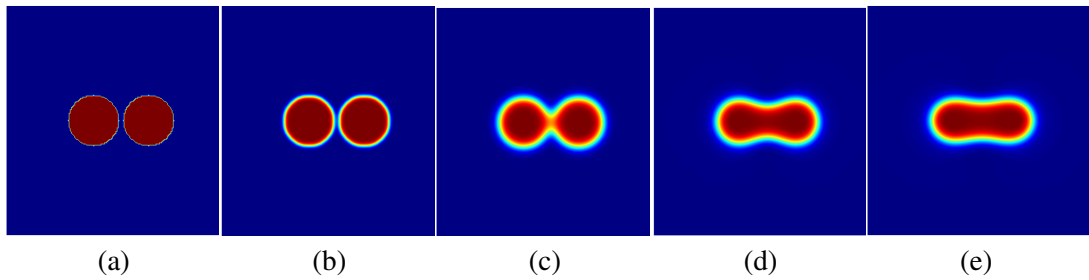


FIGURE 3. (a) is initial condition with two circle shape, (b) is $\gamma = 0.1$, (c) is $\gamma = 0.01$, (d) is $\gamma = 0.001$, (e) is $\gamma = 0$.

5. CONCLUSION

From this work, we presented the relation of the semi implicit Euler's and the linear stabilized schemes using the DP method. Using the numerical simulation, we verified the order of space and time in a one dimensional space. In addition, we presented the mass preserving and the energy dissipation properties in a two dimensional space. Moreover, the relation of the viscous CH equation and unconditionally gradient stable numerical schemes for the CH equation is presented using the change of variable. The effect of the viscosity is also presented by numerical experiment.

ACKNOWLEDGES

This research was supported by "Regional Innovation Strategy (RIS)" through the National Research Foundation of Korea (NRF) funded by the Ministry of Education (MOE) (No. 2023A-02-06-01-010).

REFERENCES

- [1] J. Cahn and J. Hilliard, *Free energy of a non-uniform system*, Chemistry and Physics, **28** (1958), 258–267.
- [2] S. Lee, C. Lee, H. Lee, J. Kim, *Comparison of different numerical schemes for the Cahn–Hilliard equation*, Journal of the Korean Society for Industrial and Applied Mathematics, **17** (2013), 197–207.
- [3] S. Lee, J. Shin, *Energy stable compact scheme for Cahn–Hilliard equation with periodic boundary condition*, Computers & Mathematics with Applications, **77**(1) (2019), 189–198.
- [4] L. Cherfils, A. Miranville, S. Zelik, *On a generalized Cahn–Hilliard equation with biological application*, Discrete and Continuous Dynamical Systems-Series B, **19**(7), (2014) 20130–2026.
- [5] P. Blair, *An analysis of the fractional step method*, Journal of Computational Physics **108**(1) (1993), 51–58.
- [6] D. Eyre, *Unconditionally gradient stable time marching the Cahn–Hilliard equation*, MRS online proceedings library (OPL) **529** (1998), 39.
- [7] X. Pan, K. Kim, C. Lee, J. Choi, *A decoupled monolithic projection method for natural convection problems*, Journal Computational Physics, **314** (2016), 160–166.
- [8] X. Pan, K. Kim, C. Lee, J. Choi, *Fully decoupled monolithic projection method for natural convection problems*, Journal Computational Physics, **334** (2017), 582–606.